Trans Indian Inst Met (2023) 76(4):945–950
https://doi.org/10.1007/s12666-022-02803-2

ORIGINAL ARTICLE

NiTi/PMMA Biocomposite: in Situ Polymerization, Microstructure and Mechanical Property

Yong-Hua Li[1] · **Jun-Hui Li**[1]

Received: 26 July 2022 / Accepted: 12 October 2022 / Published online: 28 October 2022

Abstract Porous titanium alloys have been used widely in the field of hard tissue prosthesis applications. But there is a critical concern regarding the degradation of mechanical properties with the increase in porosity. A strategy of incorporating porous metal with biomedical polymethyl methacrylate (PMMA) is proposed to ameliorate the mechanical property of metal foam. In this literature, porous NiTi shape memory alloy (SMA) has been fabricated by combustion synthesis. NiTi/PMMA biocomposite has been prepared by soaking the porous NiTi SMA sample in the mixture of monomer MMA solutions and initiator AIBN with weight ratio 100:1 and then evacuating to 0.08 MPa for 1 h followed by polymerization at 319 K in air for 24 h. The permeable porous structure favors the filling of pores with PMMA. The compressive strength of NiTi/PMMA composite has been significantly enhanced compared with that of porous NiTi SMA. The elastic modulus and compressive strength of biocompatible NiTi/PMMA composite match those of bone tissue.

Keywords Porous NiTi alloy · NiTi/PMMA composite · Microstructure · Mechanical property · Biomaterial

1 Introduction

It is recognized that titanium alloy has been extensively used in the field of hard tissue implantology owing to the merits of high strength and ductility, good corrosion resistance and biocompatibility [1–3]. But it is not an ideal implant candidate because there is a critical issue regarding the biomechanical incompatibility, i.e., a much higher stiffness (60 ~ 80 GPa) compared with that (≤ 27 GPa) of bone tissue.

The elastic modulus mismatch between the implant and the surrounding bone tissue may cause osteoporosis and bone resorption [1–6]. To resolve this problem, a foaming strategy enlightened by the porous architecture of cancellous bone has been proposed to reduce elastic modulus by introducing porous structure into solid metallic prosthesis [4, 5]. The new strategy spurs the research and development of porous metallic prosthesis candidates with appropriate elastic modulus, adequate strength, good corrosion resistance and excellent compatibility [7–12]. Porous Ti–Cu, Ti–Nb, Ti–Mo alloys have been fabricated by methods of powder sintering, gelcasting, microwave sintering and selective laser sintering [7–12]. Mechanical properties depend on the porosity of porous titanium alloys [7–9]. The in vivo implantation experiments of sintered porous Ti–Nb–Zr alloys indicated that they exhibited good biocompatibility with respect to osteoinductive property [10].

As a particular type of biomedical titanium alloy, NiTi shape memory alloy (SMA) is featured by shape memory effect (SME) and superelasticity (SE) although the effect of released nickel ion on the allergy reaction is still controversial. SME and SE are associated with thermoelastic and stress-induced martensitic transformation, respectively. SME is a plastic strain given at a temperature below the start temperature of reverse martensitic transformation (*As*) and recovers by heating to a temperature above the finish temperature of reverse martensitic transformation (A_f). SE occurs at a temperature above A_f, causing a stress-induced martensitic transformation upon loading and by the subsequent reverse transformation upon unloading [13, 14].

✉ Yong-Hua Li
yhlicn@163.com

[1] School of Materials Science and Engineering, Shenyang Ligong University, Shenyang 110159, People's Republic of China

Furthermore, porous NiTi SMA has attracted considerable attention due to the porous structure. Some reports have focused on the fabrication, microstructure, mechanical properties, corrosion behavior and in vitro/*vivo* biocompatibility evaluations of porous NiTi SMA [15–29]. Among various manufacturing routes, the widely utilized self-propagating high-temperature synthesis (SHS) or combustion synthesis possesses distinct advantages over powder metallurgy, space holder sintering, microwave sintering and selective laser sintering, including low capital investment, simplicity, good maneuverability, wide porosity range, saving time, etc. [16–25]. The in vitro and in vivo investigation revealed that porous NiTi SMA had better osteoconductivity and osteointegration than the bulk one [17, 18]. Available studies indicate that elastic modulus, strength and corrosion resistance deteriorate or degrade dramatically with the increase in porosity of porous NiTi SMA [19–22]. It is hard for metal foam with high porosity to sustain appropriate elastic modulus and adequate strength to match those of bone tissues. It could be ascribed to increasing pore stress concentration and decreasing actual load bearing section area.

As a biomedical polymer, polymethyl methacrylate (PMMA)-based composites can be used for prosthesis applications because of good biocompatibility [30–35]. Proper elastic modulus and strength of PMMA are close to those of bones. A strategy was proposed to incorporate PMMA into porous titanium with uniform structure and lower porosity sintered from spherical titanium powders [35].

In this literature, a strategy is proposed to incorporate PMMA into porous NiTi SMA in order to ameliorate the mechanical property of the metallic scaffold. The new NiTi/PMMA biocomposite integrates PMMA into metal foam by in situ polymerization. One motivation of this literature is to fabricate NiTi/PMMA composite by polymerization of the mixtures of monomer and initiator in porous NiTi SMA prepared by SHS. The other is to investigate the microstructure and mechanical properties of porous NiTi SMA and NiTi/PMMA composite.

2 Experimental Details

2.1 SHS of Porous NiTi SMA

Commercially pure elemental Ti and Ni powders were blended according to the equiatomic ratio ($Ni_{50}Ti_{50}$) for 24 h and formed into green compacts (Φ25mm × 50 mm). The compacts placed in a furnace under the protection of flow argon were preheated to 673 K and ignited at end by electrified tungsten coil. Shining brightly, the combustion wave would propagate along the axis to the other end in a short time. The cooled porous NiTi SMA compacts were cut into samples with size of Φ8mm × 10 mm and washed using acetone and distilled water in ultrasonic cleaner in turn five times.

2.2 Polymerization of PMMA from Monomer and Initiator

The monomer MMA solution was mixed with the initiator 2,2'-azobisisobutyronitrile (AIBN) according to the weight ratio 100:1. In order to optimize the polymerization temperature, the mixed solutions poured into glass tube with inner diameter of 10 mm were polymerized in air at 309, 319 and 335 K for 24 h, respectively.

2.3 Fabrication of NiTi/PMMA Composite

A set of cleaned and dried porous samples were soaked in the above-mentioned solutions and then polymerized at 319 K in air for 24 h. For comparative purpose, another set of samples immersed in the mixed solutions at ambient temperature were evacuated to pressure of 0.08 MPa for 1 h before polymerization.

2.4 Characterization

Phase compositions of porous NiTi SMA were determined using X-ray diffraction (XRD, Rigaku Ultima IV diffractometer). Microstructure observations were performed on scanning electron microscope (SEM, Hitachi S-3400 N), equipped with energy dispersion spectrum (EDS). Molecule structure of PMMA was measured on Fourier transformation infrared spectroscopy (FTIR, Nocolet iS50). Compressive properties were investigated using compression experiments on samples with dimensions of Φ10mm × 12 mm at strain rate of $10^{-3}S^{-1}$. Porosity measurement method was described elsewhere [7].

3 Results and Discussion

3.1 Porous NiTi SMA

Figure 1 shows the XRD patterns of porous NiTi SMA prepared by SHS. It consists of intermetallic phases like TiNi (B2), Ti_2Ni and $TiNi_3$, with B2 being the major phase. Momentary synthesis and cooling in water would retain the parent phase B2 and retard formation of martensite B19'. According to the Ni–Ti binary phase diagram, it is impossible to obtain NiTi SMA entirely without other intermetallics because the Gibbs free energy of Ti_2Ni and $TiNi_3$ is lower than that of NiTi phase.

As illustrated in Fig. 2a, the pore morphology of porous NiTi SMA with porosity of 64% fabricated by SHS exhibits

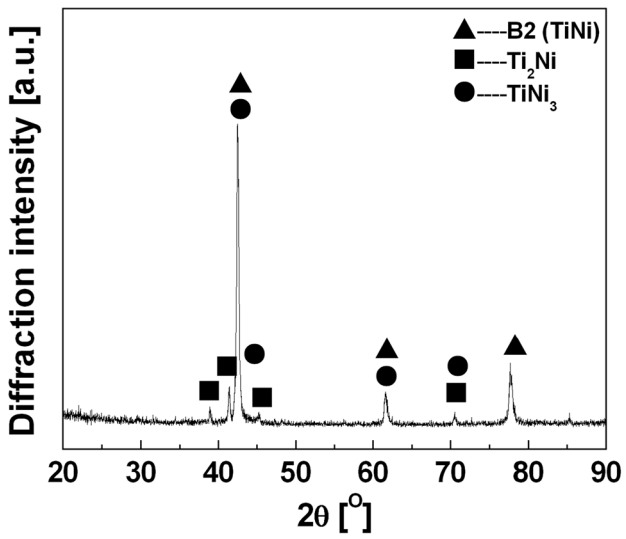

Fig. 1 XRD patterns of porous NiTi SMA

homogeneous, permeable and 3D-interconnected porous architecture with mean pore size 236 μm.

3.2 Preparations of PMMA and NiTi/PMMA Composite

The mixed solution intended to polymerization at lower temperature 309 K is still in liquid state within 24 h. The PMMA sample polymerized at 319 K exhibits transparent and pore-free appearance, as presented in Fig. 3a, while the sample polymerized at higher temperature 335 K is characterized by explosive polymerization, as illustrated in Fig. 3b. These comparative experiments indicate that the proper polymerization temperature of PMMA from MMA and AIBN with weight ratio 100:1 is 319 K.

Figure 3(c and d) presents the photographs of NiTi/PMMA composite developed by different procedures. As shown in Fig. 3c, the sample has solidified completely without any air bubble when the porous NiTi alloy soaked in the

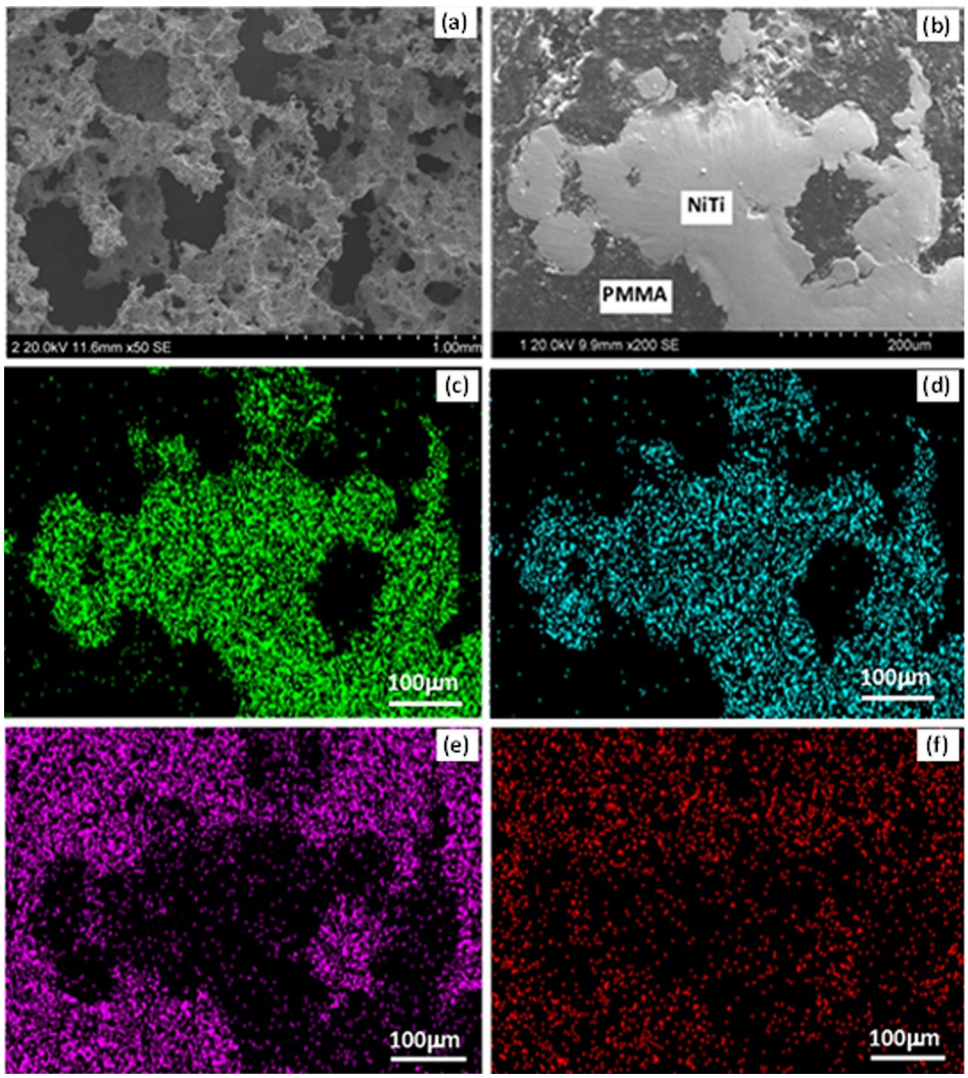

Fig. 2 SEM photographs for pore morphology of **a** porous NiTi SMA with porosity 64%; **b** NiTi/PMMA composite; EDS results for distributions of titanium **c**, nickel **d**, carbon **e** and oxygen **f** on the surface of NiTi/PMMA composite

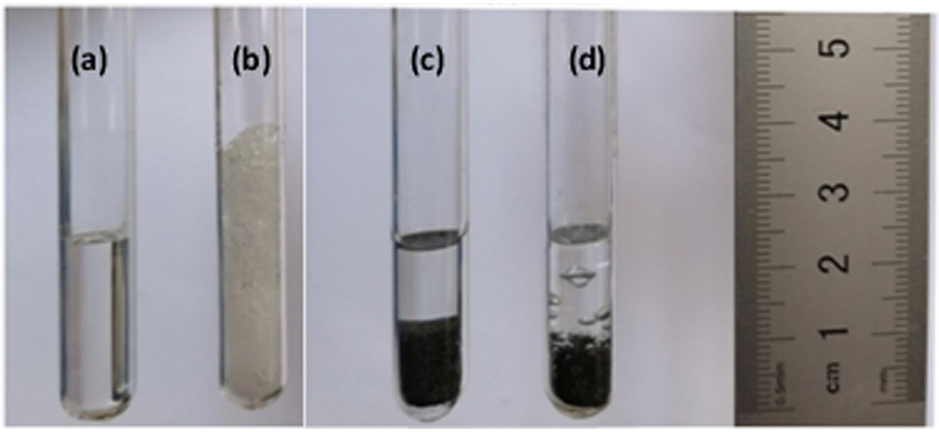

Fig. 3 Photographs of PMMA samples: **a** optimal polymerization and **b** explosive polymerization; NiTi/PMMA composite: **c** optimal sample and **d** sample with air bubbles

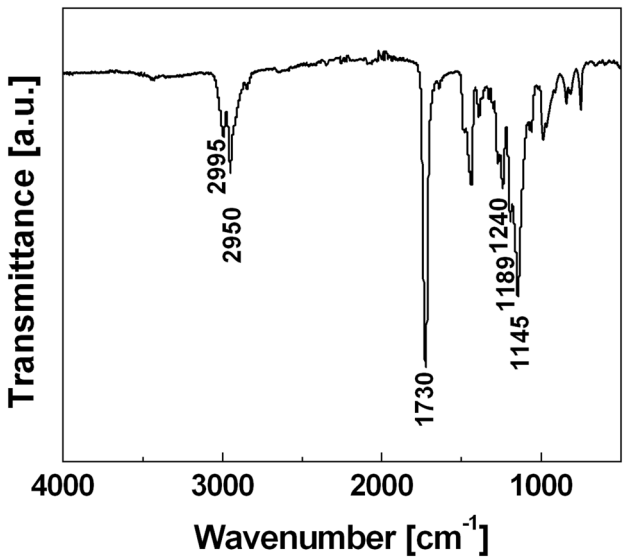

Fig. 4 FTIF spectrum of PMMA

above mixed solutions was evacuated and in situ polymerized in air at 319 K for 24 h. As presented in Fig. 3d, some air bubbles exist in the solidified sample when the porous alloy was immersed in the above solution and directly polymerized. The comparative investigations reveal that the evacuation is a prerequisite procedure before polymerization to eliminate the air existing in the pores of metallic foam.

3.3 NiTi/PMMA Composite

Figure 4 presents the FTIR spectrum in the wave number region between 4000 and 500 cm^{-1} of PMMA. The stretching vibration peaks at 2995 and 2950 cm^{-1} correspond to the methyl and methylene groups, respectively. Furthermore, the strong stretching vibration peak at 1730 cm^{-1} represents the carbonyl group, being a typical band of PMMA. Moreover, the stretching vibration peaks at 1240, 1189 and 1145 cm^{-1} are associated with the ether groups. In general, the FTIR spectrum exhibits the typical characteristics of PMMA, being similar to the reported information [36].

Figure 2b shows the SEM image of the morphology for cross section of NiTi/PMMA composite. NiTi matrices are surrounded by irregular shaped PMMA, which is previously occupied by pores. As illustrated in Fig. 2(c to f), EDS results for the distributions of titanium (Ti), nickel (Ni), carbon (C) and oxygen (O) on surface of NiTi/PMMA composite reveal that C and O-rich substances distribute predominately in pores whereas Ni and Ti–rich mainly in NiTi SMA. The EDS together with FTIR investigations confirm the existence of PMMA product. The permeable porous structure favors filling of pores with PMMA. Consequently, the amount of nickel ions released from NiTi SMA would be reduced remarkably because the alloy is mostly penetrated and filled by PMMA. Actually, NiTi/PMMA composite possesses biochemical compatibility because it is prepared from biocompatible PMMA and porous NiTi SMA at low polymerization temperature without other chemical reaction and metallurgical process.

Figure 5 depicts the nominal stress–strain curves of NiTi/PMMA composite and porous NiTi SMA under compression load. During the compression process, they undergo stages of elastic deformation, plastic deformation and fracture.

Elastic modulus and compressive strength could be determined by the slope coefficient from the initial elastic portion and stress peak value, respectively. As listed in Table 1, there is a remarkable enhancement in compressive strength for NiTi/PMMA composite compared with porous NiTi SMA with porosity 64% because the actual load area is enhanced significantly by the filling of pores with the polymer. Furthermore, NiTi/PMMA composite and porous NiTi SMA possess close elastic modulus. This phenomenon can be ascribed to the close stiffness between porous NiTi SMA with porosity 64% and PMMA. The biocomposite has higher strength and lower stiffness. Consequently, NiTi/PMMA composite has better biomechanical compatibility because

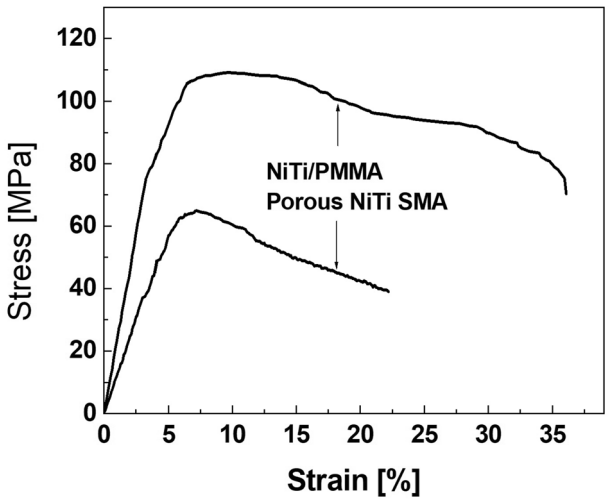

Fig. 5 Stress–stain curves of NiTi/PMMA composite and porous NiTi SMA under compression load

Table 1 Elastic modulus and compressive strength of porous NiTi SMA, NiTi/PMMA composite and cancellous bone

Materials	Elastic modulus [GPa]	Compressive strength [MPa]
NiTi SMA [porosity 64%]	1.2 ± 0.3	65 ± 6
NiTi/PMMA	2.3 ± 0.4	109 ± 8
Cancellous bone	1 ~ 2 [5]	1 ~ 100 [5]

the matching of mechanical property between the composite and cancellous bone. Therefore, NiTi/PMMA composite is expected to be ideal hard tissue implant candidate with respect to biochemical and biomechanical compatibility.

It should be stated that the implantation investigations of NiTi/PMMA composite are needed to clarify its in vivo biocompatibility in the future.

4 Conclusions

Based on the preparation, microstructure and mechanical properties of porous NiTi SMA and NiTi/PMMA composite, the following conclusions could be drawn:

(a) The optimal synthesis procedure of PMMA is the polymerization of mixture of monomer MMA solution and initiator AIBN with weight ratio 100:1 at 319 K in air within 24 h.
(b) NiTi/PMMA composite has been successfully fabricated by soaking porous NiTi SMA in the mixed solutions and evacuating to pressure 0.08 MPa for 1 h at ambient temperature followed by polymerization.
(c) Distinct enhancement in compressive strength of NiTi/PMMA composite compared with porous NiTi SMA reveals that the strategy of integration of PMMA into porous NiTi SMA is effective to ameliorate its mechanical property.
(d) Compressive strength and elastic modulus of NiTi/PMMA composite match those of bone tissue.

Acknowledgements This work was supported by the financial supports from Natural Science Foundation of Liaoning Province in China (Grant No. 2019–ZD–0257).

Declarations

Conflict of interest The authors have no conflicts of interest to declare that are relevant to the content of this article.

References

1. Kaur M, and Singh K, *Mater Sci Eng C* **102** (2019) 844.
2. Chen Q, and Thouas AG, *Mater Sci Eng R* **87** (2015) 1.
3. Geetha M, Singh A K, Asokamani R, and Gogia A K, *Prog Mater Sci* **54** (2009) 397.
4. Gibson L J, and Ashby M F, *Cellular Solids: Structure and Properties*, Cambridge University Press, Cambridge, (1988).
5. Suchanek W, and Yoshimura M, *J Mater Res* **13** (1998) 94.
6. Hench L L, and Ethripge E C, *Biomaterial: An interfacial Approach*, Academic Press, New York, (1982).
7. Li Y H, Chen N, Cui H T, and Wang F, *J Alloys Compd* **723** (2017) 967.
8. Yang D, Guo Z, Shao H, Liu X, and Ji Y, *Procedia Eng* **36** (2012) 160.
9. Xie F, He X, Lv Y, Wu M, He X, and Qu X, *Corro Sci* **95** (2015) 117.
10. Maya A E A, Grana D R, Hazarabedian A, Kokubu G A, Luppo M I, and Vigna G, *Mater Sci Eng C* **32** (2012) 321.
11. Fojt J, Joska L, and Málek J, *Corro Sci* **71** (2013) 78.
12. Prakash C, Singh S, Ramakrishna S, Królczyk G, and Le C H, *J Alloys Compd* **824** (2020) 153774.
13. Otsuka K and Ren X, *Intermetallics* **7** (1999) 511.
14. Jani J M, Leary M, Subic A and Gibson M A, *Mater Design* **56** (2014) 1078.
15. Biesiekierski A, Wang J, Gepreel M A H, and Wen C, *Acta Biomater* **8** (2012) 1661.
16. Bansiddhi A, Sargeant T D, Stupp S I, and Dunand D C, *Acta Biomater* **4** (2008) 773.
17. Zhu S L, Yang X J, Chen M F, Li C Y, and Cui Z D, *Mater Sci Eng C* **28** (2008) 1271.
18. Liu X, Wu S, Yeung K W K, Chan Y L, Hu T, Xu Z, Liu X, Chung J C Y, Cheung K M C and Chu P K, *Biomaterials* **32** (2011) 330.
19. Itin V I, Gyunter V E, Shabalovskaya S A, and Sachdeva R L C, *Mater Charact* **32** (1994) 179.
20. Li Y H, Rong L J and Li Y Y, *J Alloys Compd* **345** (2002) 271.
21. Andani M T, Saedi S, Turabi A S, Karamooz M R, Haberland C, Karaca H E and Elahinia M, *J Mech Behav Biomed Mater 68* (2017) 224.
22. Li Y H, Rao G B, Rong L J, and Li Y Y, *Mater Lett* **57** (2002) 448.
23. Gunther V, Yasenchuk Y, Chekalkin T, Marchenko E, Gunther S, Baigonakova G, Hodorenko V, Kang J, Weiss S, and Obrosov A, *Adv Powder Technol* **30** (2019) 673.

24. Resnina N, Belyaev S, Voronkov A, and Badun R, *Mater Today Proc* **4** (2017) 4690.
25. Tosun G, Orhan N, and Özler L, *Mater Lett* **66** (2012) 138.
26. Ma X, Wang H, Xie H, Qu J, Chen X, Chen F, Song Q, and Yin H, *J Alloys Compd* **794** (2019) 455.
27. Peng W, Liu K, Shah B A, Yuan B, Gao Y, and Zhu M, *J Alloys Compd* **816** (2020) 152578.
28. Zhu S, Bouby C, Cherouat A, and Zineb T, *Int J Solids Struct* **168** (2019) 109.
29. Tang C Y, Zhang L N, Wong C T, Chan K C, and Yue T M, *Mater Sci Eng A*, **528** (2011) 6006.
30. Archana R, Baldia M, Jeeva JB, kumar D, and Joseph M, *Mater Today Proc* **15** (2019)167.
31. Topouzi M, Kontonasaki E, Bikiaris D, Papadopoulou L, Paraskevopoulos K M, and Koidis P, *J Mech Behav Biomed Mater* **69** (2017) 213.
32. Saji G S, Shamnadh M, Varma S, Amanulla S, and Bharath R S, *Mater Today Proc* **5** (2018)16509.
33. Ananthu M, Shamnadh M, and Dileep P N, *Mater Today Proc* **5** (2018) 25657.
34. Chen L, Tang Y, Zhao K, Zha X, Liu J, Bai H, and Wu Z, *Colloid Surf. B* **183** (2019) 110448.
35. Nakai M, Niinomi M, Akahori T, Tsutsumi H, Itsuno S, Haraguchi N, Itoh Y, Ogasawara T, Onishi T, and Shindoh T, *J Mech Behav Biomed Mater* **3** (2010) 41.
36. Reddy M R, Subrahmanyam A R, Reddy M M, Kumar J S, Kamalaker V, and Reddy M J, *Mater Today Proc* **3** (2016) 3713.